Regional Differences in the Binding of Selective Muscarinic Receptor Antagonists in Rat Brain: Comparison with Minimum-Energy Conformations

William S. Messer, Jr.,* Brenda R. Ellerbrock, Douglas A. Smith,† and Wayne Hoss

Department of Medicinal and Biological Chemistry, College of Pharmacy, and Department of Chemistry, University of Toledo, 2801 W. Bancroft St., Toledo, Ohio 43606. *Received August 17, 1988*

The binding of selective muscarinic receptor antagonists to regions of rat brain was examined through quantitative autoradiographic techniques. 5,11-Dihydro-11-[(4-methyl-1-piperazinyl)acetyl]-6*H*-pyrido[2,3-*b*][1,4]benzodiazepin-6-one [pirenzepine (compound I)] and 11-[[2-[(diethylamino)methyl]-1-piperidinyl]acetyl]-5,11-dihydro-6*H*-pyrido[2,3-*b*][1,4]benzodiazepin-6-one [AF-DX 116 (compound II)] were chosen on the basis of their selectivity for M_1 and M_2 muscarinic receptors, respectively, and similarities in chemical structure. Pirenzepine displayed a higher potency than II for inhibition of [^{3}H]-*l*-quinuclidinyl benzilate ([^{3}H]-*l*-QNB) binding to rat brain sections. Scatchard analyses of binding to brain sections revealed heterogeneous binding profiles for both antagonists, suggesting the presence of multiple receptor binding sites. Quantitative autoradiographic techniques were utilized in regional analyses of antagonist binding. Pirenzepine displayed the highest affinity for hippocampal, striatal, and amygdaloid muscarinic receptors (IC_{50} values less than 0.4 μM), with a slightly lower affinity for cortical receptors (IC_{50} values between 0.4 and 0.8 μM). Pirenzepine displayed the lowest affinity for thalamic and brainstem regions with IC_{50} values generally greater than 1.0 μM. In contrast, II bound with higher affinity to muscarinic receptors in brainstem, cerebellar, and hypothalamic nuclei (IC_{50} values less than 0.5 μM) than to receptors in thalamic nuclei (IC_{50} values between 0.5 and 2.0 μM). Binding sites with the lowest affinity for II were found in cortical, striatal, and hippocampal regions (IC_{50} values greater than 2.0 μM). The binding profiles of the two selective muscarinic antagonists reveal the complexity and diversity of muscarinic receptor subtypes throughout the brain. The data provide a basis for identifying muscarinic receptor subtypes (as defined through cloning procedures) with selective ligands. Minimum-energy conformations of pirenzepine and II were calculated by using the program MacroModel (version 2.0). Pirenzepine displayed three energy minima, differing in the relative position of the piperazine ring with respect to the tricyclic system. In contrast, the (diethylamino)methyl substituent on the piperidine ring conferred a much larger set of minimum-energy conformations on II. It is suggested that the greater conformational flexibility of the side chain allows II to achieve a conformation inaccessible to pirenzepine, which allows it to bind preferentially to M_2 receptors.

The binding of selective antagonists to muscarinic receptors has led to the proposed subclasses designated M_1 and M_2.[1] 5,11-Dihydro-11-[(4-methyl-1-piperazinyl)-acetyl]-6*H*-pyrido[2,3-*b*][1,4]benzodiazepin-6-one [pirenzepine (I)] displays a selectivity for M_1 receptors found predominantly in the forebrain[2] while both 11-[[2-[(diethylamino)methyl]-1-piperidinyl]acetyl]-5,11-dihydro-6*H*-pyrido[2,3-*b*][1,4]benzodiazepin-6-one [AF-DX 116 (II)] and gallamine bind selectively to M_2 receptors in the heart and brain stem.[3-6] Autoradiographic studies indicate that the distribution of high-affinity gallamine sites and high-affinity agonist sites is similar,[7-9] while high-affinity pirenzepine sites appear to correspond to low-affinity carbamylcholine (and gallamine) sites.[8,10-12]

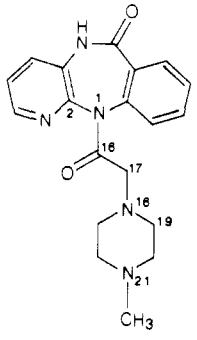

I

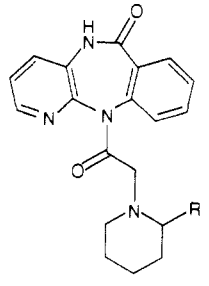

II: R = $CH_2N(CH_2CH_3)_2$
III: R = CH_3

Recent studies utilizing selective ligands have identified functional and anatomical differences within the M_2 receptor subtype.[13] Receptors with high affinity for II and low affinity for pirenzepine have been labeled cardiac M_2 receptors, while those with low affinity for both pirenzepine and II have been called either glandular M_2 receptors or, more recently, M_3 receptors.[14]

Within the past 2 years, cDNA cloning techniques have been utilized to identify several different muscarinic receptors.[15-19] On the basis of different sequences for the muscarinic receptors Bonner and colleagues[18] proposed that at least four subtypes could be identified within the central nervous system. The assignment of the codes m_1, m_2, m_3, and m_4 to the receptors, although not based strictly on the prior information relating to the selectivity of pirenzepine for muscarinic receptors, provides a useful ca-

† Department of Chemistry.

(1) Hammer, R.; Giachetti, A. *Life Sci.* **1982**, *31*, 2991.
(2) Hammer, R.; Berrie, C. P.; Birdsall, N. J. M.; Burgen, A. S. V.; Hulme, E. C. *Nature* **1980**, *283*, 90.
(3) Ellis, J.; Hoss, W. *Biochem. Pharmacol.* **1982**, *31*, 873.
(4) Stockton, J. M.; Birdsall, N. J. M.; Burgen, A. S. V.; Hulme, E. C. *Mol. Pharmacol.* **1983**, *23*, 551.
(5) Burke, R. E. *Mol. Pharmacol.* **1986**, *30*, 58.
(6) Hammer, R.; Giraldo, E.; Schiavi, G. B.; Monferini, E.; Ladinsky, H. *Life Sci.* **1986**, *38*, 1653.
(7) Wamsley, J. K.; Zarbin, M. A.; Birdsall, N. J. M.; Kuhar, M. J. *Brain Res.* **1980**, *200*, 1.
(8) Cortés, R.; Palacios, J. M. *Brain Res.* **1986**, *362*, 227.
(9) Price, M.; Messer, W. S., Jr.; Hoss, W. *Biochem. Pharmacol.* **1986**, *35*, 4171.
(10) Wamsley, J. K.; Gehlert, D. R.; Roeske, W. R.; Yamamura, H. I. *Life Sci.* **1984**, *34*, 1395.
(11) Messer, W. S., Jr.; Hoss, W. *Brain Res.* **1987**, *407*, 27.
(12) Mash, D. C.; Potter, L. T. *Neuroscience* **1986**, *19*, 551.
(13) Giraldo, E.; Hammer, R.; Ladinsky, H. *Life Sci.* **1987**, *40*, 833.
(14) Doods, H. N.; Mathy, M.-J.; Davidsko, D.; van Charldorp, K. J.; de Jonge, A.; van Zwieten, P. A. *J. Pharmacol. Exp. Ther.* **1987**, *242*, 257.
(15) Kubo, T.; Maeda, A.; Sugimoto, K.; Akiba, I.; Mikami, A.; Takahashi, H.; Haga, T.; Haga, K.; Ichiyama, A.; Kangawa, K.; Matsuo, H.; Hirose, T.; Numa, S. *FEBS Lett.* **1986**, *209*, 367.
(16) Kubo, K.; Fukuda, K.; Mikami, A.; Maeda, A.; Takahashi, H.; Mishina, M.; Haga, T.; Haga, K.; Ichiyama, A.; Kangawa, K.; Kojima, M.; Matsuo, H.; Hirose, T.; Numa, S. *Nature* **1986**, *323*, 411.
(17) Peralta, E. G.; Winslow, J. W.; Peterson, G. L.; Smith, D. H.; Ashkenazi, A.; Ramachandran, J.; Schimerlik, M. I.; Capon, D. J. *Science* **1987**, *236*, 600.
(18) Bonner, T. I.; Buckley, N. J.; Young, A. C.; Brann, M. R. *Science* **1987**, *237*, 527.

0022-2623/89/1832-1164$01.50/0

Table I

A. Inhibition of QNB Binding by Pirenzepine and II in Rat Forebrain

forebrain regions	pirenzepine		compound II		
	IC_{50}, μM	Hill slope	IC_{50}, μM	Hill slope	ratio[b]
cerebral cortex layers I–III	0.44 ± 0.06	0.76 ± 0.06	1.9 ± 0.47	0.76 ± 0.09	4.3
cerebral cortex layers IV and V	0.48 ± 0.05	0.76 ± 0.04	2.9 ± 0.67	0.73 ± 0.11	6.0
cerebral cortex layer VI	0.52 ± 0.07	0.85 ± 0.07	4.9 ± 1.06	0.68 ± 0.09	9.4
primary olfactory cortex	0.17 ± 0.01	0.70 ± 0.03	4.3 ± 0.90	0.41 ± 0.01	25.3
retrosplenial cortex	0.46 ± 0.04	0.98 ± 0.07	1.6 ± 0.36	0.79 ± 0.12	3.5
anterior cingulate cortex	0.71 ± 0.08	0.80 ± 0.08	6.5 ± 2.45	0.61 ± 0.11	9.2
posterior cingulate cortex	0.79 ± 0.02	1.11 ± 0.14	3.2 ± 0.45	1.08 ± 0.23	4.1
entorhinal cortex	0.24 ± 0.07	0.82 ± 0.17	2.3 ± 1.47	0.95 ± 0.38	9.6
dentate gyrus	0.19 ± 0.00	0.95 ± 0.09	7.0 ± 0.82	0.73 ± 0.14	36.8
ventral dentate gyrus	0.21 ± 0.04	0.98 ± 0.14	2.1 ± 0.86	0.49 ± 0.00	10.0
hippocampus CA1	0.29 ± 0.02	0.93 ± 0.06	6.1 ± 1.34	0.95 ± 0.29	21.0
hippocampus CA3	0.27 ± 0.02	0.83 ± 0.05	6.3 ± 1.24	0.60 ± 0.08	23.3
hippocampus CA4	0.29 ± 0.05	0.90 ± 0.04	3.2 ± 0.50	0.68 ± 0.08	11.0
subiculum	0.41 ± 0.07	0.79 ± 0.09	1.8 ± 0.37	0.56 ± 0.06	4.4
ventral subiculum	0.42 ± 0.05	0.85 ± 0.04	4.0 ± 1.81	0.54 ± 0.08	9.5
caudate nucleus	0.31 ± 0.05	0.75 ± 0.04	5.8 ± 2.23	0.63 ± 0.04	18.7
neostriatum	0.79 ± 0.11	0.85 ± 0.05	14.0 ± 4.35	0.47 ± 0.08	17.7
lateral amygdaloid nucleus	0.33 ± 0.06	0.82 ± 0.10	4.3 ± 1.07	0.67 ± 0.07	13.0
basolateral amygdaloid nucleus	0.45 ± 0.12	0.91 ± 0.12	7.3 ± 1.92	0.50 ± 0.06	16.2
central amygdaloid nucleus	0.43 ± 0.08	0.85 ± 0.11	9.8 ± 5.7	0.36 ± 0.03	22.8
medial amygdaloid nucleus	0.23 ± 0.01	0.78 ± 0.07	1.4 ± 0.56	0.49 ± 0.05	6.1

B. Inhibition of QNB Binding by Pirenzepine and II in Rat Midbrain[a,c]

midbrain regions	pirenzepine		compound II		
	IC_{50}, μM	Hill slope	IC_{50}, μM	Hill slope	ratio[b]
anterior hypothalamus	1.4 ± 0.74	0.74 ± 0.06	2.0 ± 1.28	0.60 ± 0.10	1.4
ventromedial hypothalamus	1.6 ± 0.96	1.10 ± 0.22	1.4 ± 0.68	0.45 ± 0.11	0.9
dorsomedial hypothalamus	2.5 ± 0.94	1.04 ± 0.24	0.61 ± 0.05	0.81 ± 0.06	0.2
laternal hypothalamus	0.50 ± 0.05	0.63 ± 0.02	0.32 ± 0.01	0.53 ± 0.10	0.6
posterior hypothalamus	1.4 ± 0.68	0.88 ± 0.10	0.49 ± 0.13	0.87 ± 0.12	0.4
zona inserta	0.52 ± 0.08	0.64 ± 0.10	0.42 ± 0.08	0.55 ± 0.02	0.8
lateral septal nucleus	0.71 ± 0.16	0.70 ± 0.06	0.84 ± 0.34	0.57 ± 0.08	0.8
bed nucleus stria terminalis	0.44 ± 0.06	0.67 ± 0.04	1.2 ± 0.43	0.59 ± 0.05	2.7
paraventricular thalamic nucleus	1.3 ± 0.31	1.25 ± 0.35	0.62 ± 0.32	0.59 ± 0.02	0.5
central medial thalamic nucleus	1.1 ± 0.19	1.04 ± 0.16	1.3 ± 0.42	0.69 ± 0.11	1.2
rhomoboid thalamic nucleus	2.0 ± 0.29	1.33 ± 0.05	2.1 ± 0.29	0.60 ± 0.00	1.1
reuniens thalamic nucleus	1.9 ± 0.33	0.80 ± 0.05	1.0 ± 0.58	0.43 ± 0.18	0.5
medial dorsal thalamic nucleus	0.68 ± 0.16	0.74 ± 0.00	1.7 ± 0.70	0.57 ± 0.07	2.5
lateral dorsal thalamic nucleus	1.4 ± 0.37	0.84 ± 0.09	1.3 ± 0.43	0.52 ± 0.10	0.9
lateral posterior thalamic nucleus	1.1 ± 0.15	1.09 ± 0.16	0.57 ± 0.10	0.74 ± 0.07	0.5
posterior thalamic nucleus	0.85 ± 0.09	1.05 ± 0.11	1.0 ± 0.17	0.71 ± 0.03	1.2
reticular thalamic nucleus	0.61 ± 0.07	0.83 ± 0.08	1.5 ± 0.64	0.54 ± 0.05	2.5
ventral posterior thalamic nucleus	0.34 ± 0.06	1.12 ± 0.30	0.86 ± 0.29	0.85 ± 0.10	2.5
dorsal lateral geniculate	0.48 ± 0.03	1.17 ± 0.23	0.72 ± 0.20	0.64 ± 0.02	1.5
ventral lateral geniculate	0.64 ± 0.13	0.85 ± 0.15	0.58 ± 0.22	0.46 ± 0.04	0.9
medial geniculate	0.54 ± 0.06	1.07 ± 0.18	0.79 ± 0.24	0.92 ± 0.17	1.5
superior colliculus	2.0 ± 0.26	1.29 ± 0.27	0.43 ± 0.08	0.78 ± 0.07	0.2
superior colliculus, infragranular	1.4 ± 0.17	1.14 ± 0.30	0.42 ± 0.07	1.15 ± 0.16	0.3
substantia nigra	0.27 ± 0.06	0.55 ± 0.06	0.58 ± 0.08	0.85 ± 0.12	2.1
periaqueductal grey	1.0 ± 0.08	1.05 ± 0.16	0.46 ± 0.09	0.99 ± 0.19	0.5

C. Inhibition of QNB Binding by Pirenzepine and II in Rat Hindbrain[a,c]

hindbrain regions	pirenzepine		compound II		
	IC_{50}, μM	Hill slope	IC_{50}, μM	Hill slope	ratio[b]
dorsal raphe nucleus	1.1 ± 0.27	0.91 ± 0.00	0.49 ± 0.15	0.91 ± 0.09	0.4
medial raphe nucleus	0.82 ± 0.44	0.70 ± 0.07	0.69 ± 0.16	1.13 ± 0.17	0.8
raphe pontis	0.45 ± 0.08	1.00 ± 0.30	0.96 ± 0.66	0.58 ± 0.00	2.1
dorsal tegmentum	0.65 ± 0.15	0.79 ± 0.15	0.30 ± 0.00	0.81 ± 0.01	0.5
inferior colliculus	0.57 ± 0.06	0.87 ± 0.16	0.26 ± 0.05	0.82 ± 0.14	0.5
cuneiform nucleus	0.85 ± 0.09	0.61 ± 0.07	0.26 ± 0.03	0.87 ± 0.16	0.3
dorsal parabrachial nucleus	0.55 ± 0.05	0.95 ± 0.39	0.24 ± 0.02	0.88 ± 0.06	0.4
ventral parabrachial nucleus	0.42 ± 0.10	1.05 ± 0.19	0.25 ± 0.05	0.85 ± 0.18	0.6
pontine nuclei	1.2 ± 0.25	1.32 ± 0.24	0.68 ± 0.20	0.92 ± 0.03	0.8
central gray, pons	0.60 ± 0.09	0.81 ± 0.11	0.31 ± 0.10	0.77 ± 0.05	0.5
cerebellum, lobe 1	0.90 ± 0.15	1.57 ± 0.85	0.31	0.6	0.3
cerebellum, lobe 2	0.74 ± 0.45	0.88 ± 0.19	0.25	0.52	0.3
cerebellum, lobe 3	0.90 ± 0.35	0.93 ± 0.22	0.31	0.51	0.3
cerebellum, lobe 4	0.84 ± 0.18	1.35 ± 0.39	0.23 ± 0.02	1.35 ± 0.72	0.3

[a] Values represent the means (±SEM) from three animals. [b] Ratio represents the IC_{50} for compound II and the IC_{50} for pirenzepine. [c] Large numbers indicate higher proportions of pirenzepine-sensitive sites.

tegorization for identifying subpopulations of muscarinic receptors with selective agents. Further studies have identified the four subtypes of muscarinic receptors within human tissues.[19]

Conformational analyses of pirenzepine and other muscarinic antagonists have been used to form an hypothesis identifying important structural features for action at muscarinic receptors.[20] Pirenzepine contains a basic amine within the piperazine ring which can be juxtaposed to the pyridine ring of the tricyclic ring system in a similar fashion to that found within a series of classical antimuscarinic agents,[21] suggesting that the basic nitrogen and its relationship to a conjugated ring system are important structural features for muscarinic antagonist activity. The early modeling studies provide a framework for identifying important structural features for muscarinic agents yet very little is known about the conformational constraints which render muscarinic antagonists selective for different receptor subtypes. Such information might be useful in designing ligands with higher selectivity for muscarinic receptor subtypes.

In this study, we have employed quantitative autoradiographic techniques to examine the distribution of muscarinic receptors and the selectivity of the antagonists pirenzepine and II. Molecular modeling studies have been used to examine the structures of the selective muscarinic antagonists and identify potentially important features for subtype selectivity. The two ligands are of particular interest because of their similarities in chemical structure, yet divergent selectivities for receptor subtypes. Quantification of selective antagonist binding to regions of rat brain reveals the pattern of complexity which has been suggested by recent advances in the sequencing of muscarinic receptors, but not confirmed previously by standard binding assays. The modeling data indicate that both pirenzepine and II have similar minimum-energy conformations with respect to the relationships between the tricyclic ring system and the side-chain ring. Compound II is conformationally more flexible than pirenzepine, which may contribute to its selectivity for M_2 receptors.

Results

Binding of Muscarinic Antagonists. The binding of [^{3}H]-*l*-QNB to rat brain sections was similar to that described previously.[7,9,11,25] Overall, pirenzepine was more potent than II in the inhibition of [^{3}H]-*l*-QNB binding to rat brain sections. The binding of II and pirenzepine to muscarinic receptors throughout the rat brain is shown in Figures 1–3.

Data generated from autoradiograms were analyzed to determine the levels of inhibition for each ligand within selected brain regions. From the raw data for each animal, the IC_{50} value and Hill slope were calculated for each brain region. The values then were used to determine the overall means for the group of animals used in the experiments. The Hill slopes and IC_{50} values for pirenzepine and II are shown in Table I.

Pirenzepine displayed the highest affinity for hippocampal, striatal, and amygdaloid muscarinic receptors (IC_{50} values less than 0.4 μM), with a slightly lower affinity for cortical receptors (IC_{50} values between 0.4 and 0.8 μM). Pirenzepine displayed the lowest affinity for thalamic and brain stem regions with IC_{50} values generally greater than 1.0 μM. In contrast to the binding of pirenzepine, II bound with higher affinity to muscarinic receptors in brainstem and hypothalamic nuclei (IC_{50} values less than 0.5 μM) than to receptors in thalamic nuclei (IC_{50} values between 0.5 and 2.0 μM). Binding sites with the lowest affinity for II were found in cortical, striatal, and hippocampal regions (IC_{50} values greater than 2.0 μM).

Within the hippocampus, an inverse relationship existed between the affinity of muscarinic receptors for pirenzepine and II (Figure 4). High-affinity sites for pirenzepine were found within the dentate gyrus and CA1 regions of the hippocampus, while low affinity sites for II were present in the same regions. The selectivity of hippocampal receptors for pirenzepine as compared to II was high in the hippocampus as indicated (Table I) by the ratio of the affinity for II to that found for pirenzepine. The caudate nucleus and cortical layers displayed a somewhat reduced selectivity for pirenzepine (Figure 5). Midbrain and brain stem regions (e.g., the periaqueductal gray and the superior colliculus) possessed a higher affinity for II than for pirenzepine as indicated by a ratio of affinities less than 1 (Table I; Figure 7).

A cursory inspection of the data suggested a reciprocal relationship between the affinity of muscarinic receptors for pirenzepine and II, although closer examination revealed some striking differences within discrete nuclei. For example, within the paraventricular nucleus, pirenzepine distinguished a single low-affinity site, while II bound heterogeneously as indicated by a low Hill slope (Table I). In other thalamic nuclei such as the central medial nucleus, both pirenzepine and II displayed a low affinity for muscarinic receptors. In contrast, midbrain regions such as the dorsolateral geniculate and substantia nigra possessed a relatively high affinity for both compounds as shown in Figure 6.

Minimum-Energy Conformations. Conformational minima for both the neutral and protonated species of pirenzepine were obtained. Three conformations (corresponding to three different orientations of the piperazine or piperidine ring with respect to the tricyclic ring system) were found for each system. Figure 8 shows the lowest minimum energy conformations for both pirenzepine and II. Figure 9 shows three conformational minima for pirenzepine which differ in the orientation of the piperazine ring relative to the tricyclic ring system.

Compound II consists of two optical isomers. In addition, the number of possible conformations is much greater than for pirenzepine because of the flexibility of the diethylamino side chain. Calculations on a model compound (III) with a methyl substituent on the piperidine ring in place of the (diethylamino)methyl moiety provided three conformational minima similar to those found for pirenzepine (Figure 9). The addition of the diethylamino group to these conformers (to produce II), followed by minimization of the entire structure, yielded eight to ten conformations of similar energy from each conformer of the model. The lowest minimum energy conformation for II is shown in Figure 8. The calculated energy for each optimized conformer of pirenzepine, protonated pirenzepine, and the model compound III (lacking the diethylamine moiety) are shown in Table II.

Discussion

The results from the autoradiographic studies described above provide evidence for the complex binding properties

(19) Peralta, E. G.; Ashkenazi, A.; Winslow, J. W.; Smith, D. H.; Ramachandran; Capon, D. J. *EMBO J.* **1987**, *6*, 3923–3929.
(20) Trummlitz, G.; Schmidt, G.; Wagner, H.-U.; Luger, P. *Arzneim.-Forsch./Drug Res.* **1984**, *34*, 849.
(21) Pauling, P.; Datta, N. *Proc. Natl. Acad. Sci. U.S.A.* **1980**, *77*, 708.
(22) Unnerstall, J. R.; Niehoff, D. L.; Kuhar, M. J.; Palacios, J. M. *J. Neurosci. Meth.* **1982**, *6*, 59.
(23) Lipton, M.; Still, W. C. *J. Comp. Chem.* **1988**, *9*, 343.
(24) For a more complete description of these special parameters, see the documentation for MACROMODEL version 2.0.
(25) Nonaka, R.; Moroji, T. *Brain Res.* **1984**, *296*, 295.

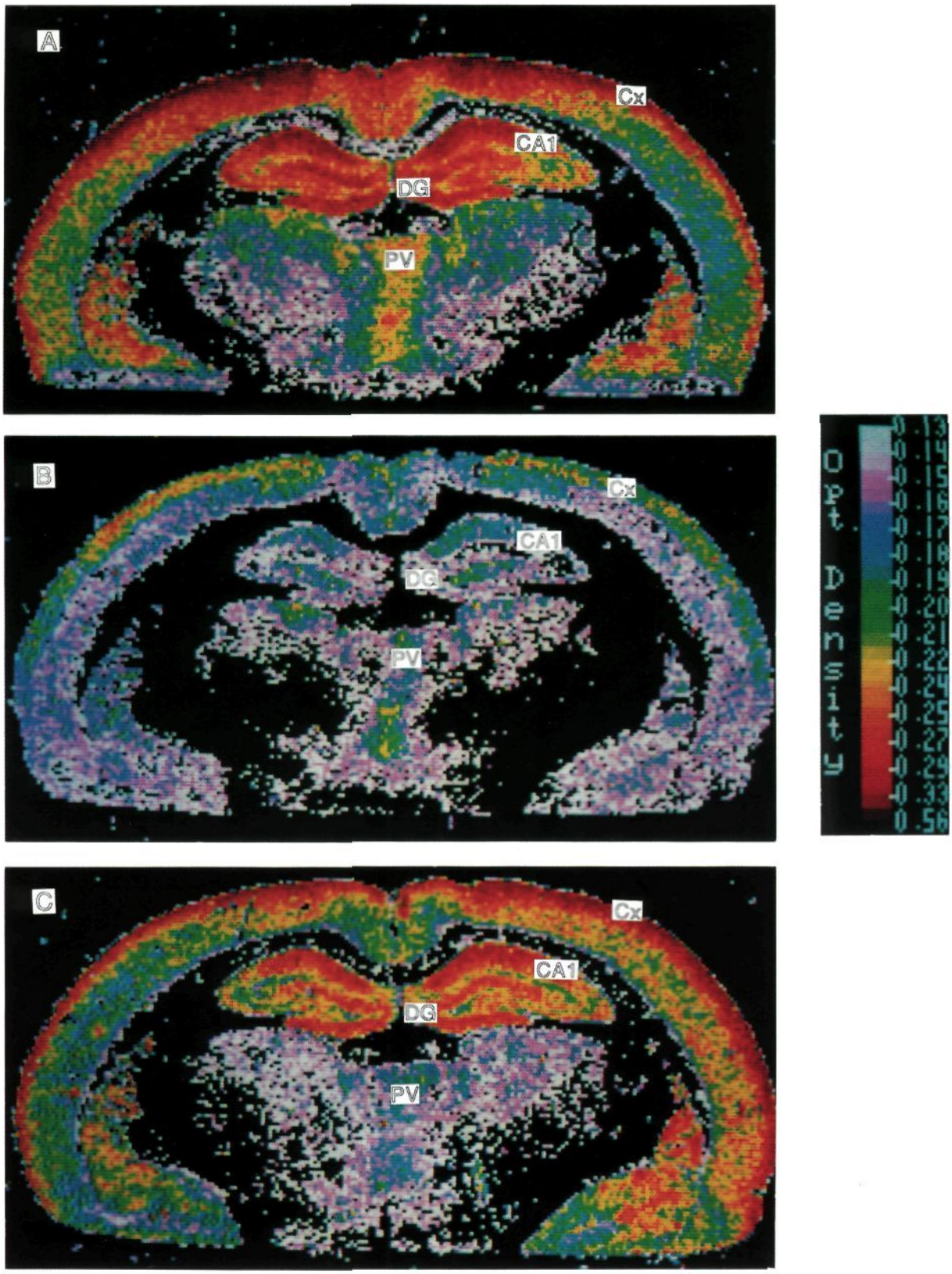

Figure 1. (A) [^{3}H]-*l*-QNB binding to muscarinic receptors at the level of the dorsal hippocampus, (B) [^{3}H]-*l*-QNB binding in the presence of 1.0 μM pirenzepine, (C) [^{3}H]-*l*-QNB binding in the presence of 1.0 μM II. Structures with detectable levels of muscarinic receptors include the cerebral cortex (Cx), dentate gyrus (DG), region CA1 of the hippocampus, and paraventricular thalamic nucleus (PV).

expected from multiple populations of muscarinic receptors. It should be noted, however, that II is racemic and it is not known which enantiomer binds to muscarinic receptors with highest affinity. Therefore, care must be taken in the interpretation of results based on differential affinities of pirenzepine and II for muscarinic receptors. Nevertheless, the data presented begin to delineate the subtypes of receptors based on regional patterns of receptor binding properties.

In the dentate gyrus, muscarinic receptors labeled by

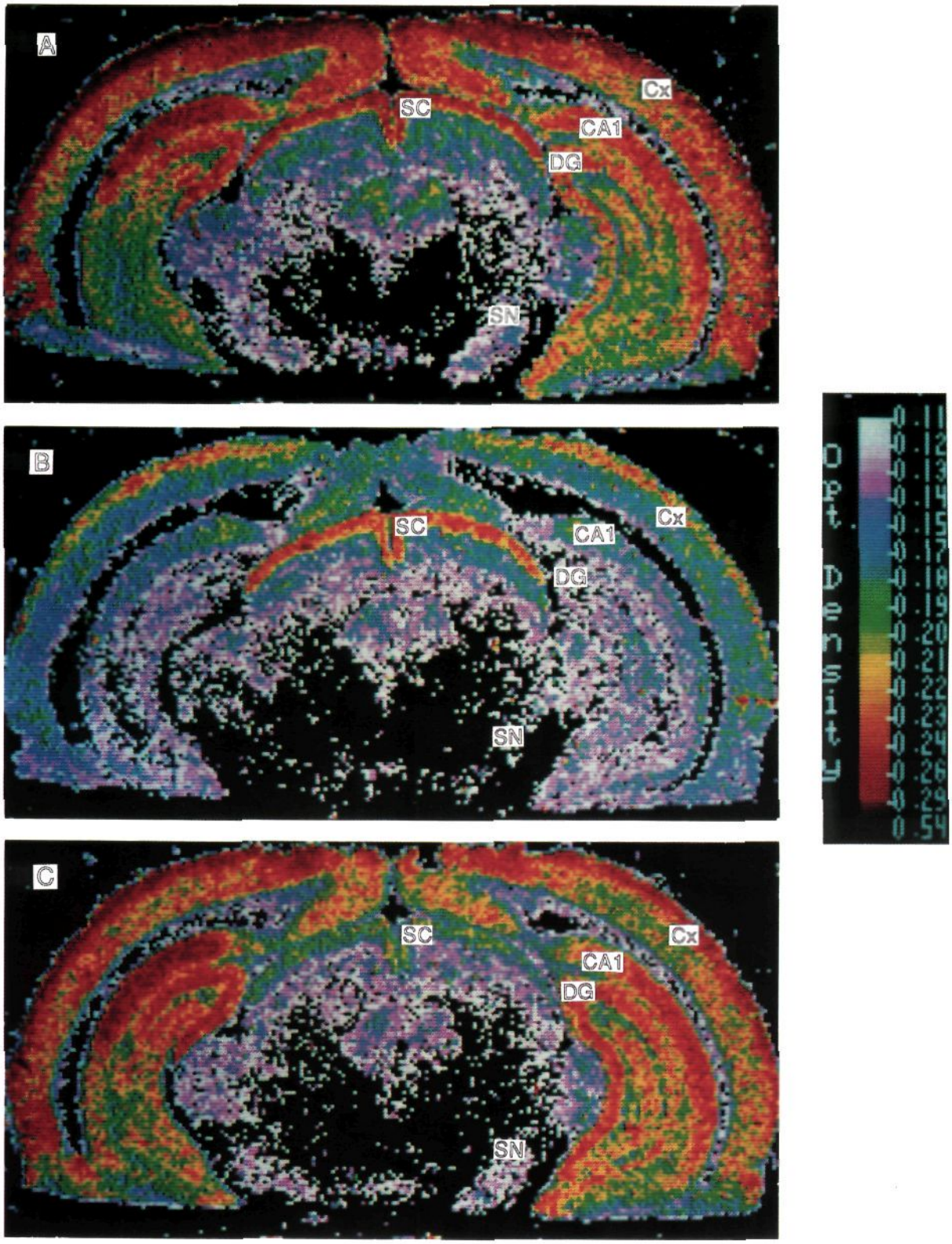

Figure 2. (A) [^{3}H]-*l*-QNB binding to muscarinic receptors at the level of the superior colliculus, (B) [^{3}H]-*l*-QNB binding in the presence of 1.0 μM pirenzepine, (C) [^{3}H]-*l*-QNB binding in the presence of 1.0 μM II. Structures with detectable levels of muscarinic receptors include the cerebral cortex (Cx), dentate gyrus (DG), region CA1 of the hippocampus, superior colliculus (SC), and substantia nigra (SN).

QNB show the highest affinity for pirenzepine and lowest affinity for II. In situ hybridization techniques, using probes generated to the mRNA for muscarinic receptor subtypes, have identified the dentate gyrus as an area with predominantly m_1 receptor mRNA, while mRNA for m_3 receptors is found in the hippocampus proper (CA1–4).[18] Bonner and colleagues[18] found that m_3 receptors expressed in COS-7 cells had a slightly lower affinity for pirenzepine than m_1 or m_4 receptors, which may explain the slighlty higher IC_{50} values within the hippocampus as compared with the dentate gyrus. The dentate gyrus muscarinic receptors may be predominantly high-affinity, pirenze-

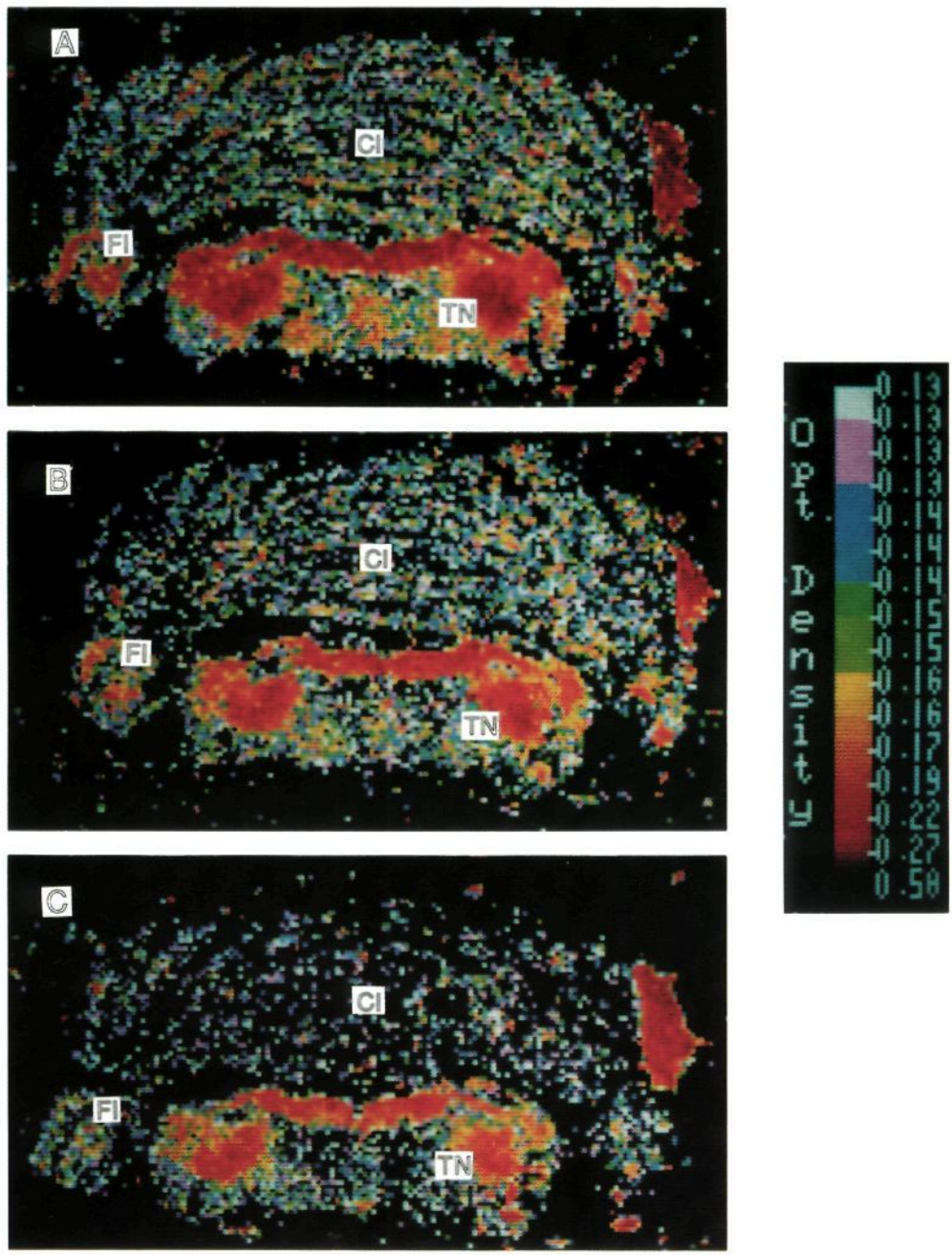

Figure 3. (A) [^{3}H]-*l*-QNB binding to muscarinic receptors at the level of the cerebellum, (B) [^{3}H]-*l*-QNB binding in the presence of 1.0 μM pirenzepine, (C) [^{3}H]-*l*-QNB binding in the presence of 1.0 μM II. Structures with detectable levels of muscarinic receptors include the cerebellar cortex (Cl), flocculus and paraflocculus (Fl), and trigeminal nucleus (TN).

pine-sensitive m_1 receptors while the CA1-4 regions may contain a mixture of m_1, m_3, and m_4 receptors.

There is evidence for presynaptic muscarinic receptors with low affinity for pirenzepine (M_2) that regulate acetylcholine release.[26,27] It is possible that presynaptic receptors are present within the hippocampus, although the high affinity displayed by pirenzepine indicates that the number of putative M_2-like presynaptic receptors is small as indicated by the inhibition curves in Figure 4.

Cortical layers possess a slightly lower affinity for pirenzepine than hippocampal layers and Hill values are generally less than unity, indicating a mixture of muscarinic receptor subtypes. It is not possible to designate the subtypes of muscarinic receptor found in the cortex, although it is likely that a mixture of at least four receptors are found in the layers of the cortex.

Compound II originally was identified as a cardioselective agent with higher potency for M_2 receptors in the heart as opposed to M_2 receptors in exocrine glands.[6] Recent evidence suggests two subtypes of M_2 receptors in brain based on differential affinities of receptors for pirenzepine and II.[13] High-affinity sites for II were found in the midbrain and brain stem regions, a finding in accord with regional binding studies using membrane preparations and with mRNA hybridization studies using probes for the m_2 (cardiac) receptor. Muscarinic receptors within the superior colliculus possess a low affinity for pirenzepine and a high affinity for II, as would be expected for m_2

(26) Mash, D. C.; Flynn, D. D.; Potter, L. T. *Science* **1985**, *228*, 1115.
(27) Meyer, E. M.; Otero, D. H. *J. Neurosci.* **1985**, *5*, 1202.

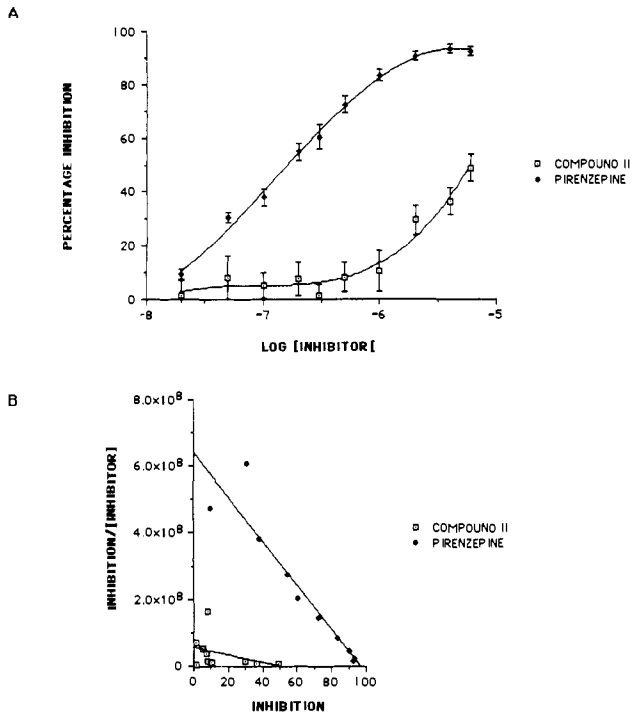

Figure 4. (A) The inhibition of [^{3}H]-*l*-QNB binding by pirenzepine and II in the dentate gyrus. Data represent the mean (±sem) from three animals with three to nine determinations for each concentration and brain region, (B) Eadie–Hofstee transformation of the data shown in 4A.

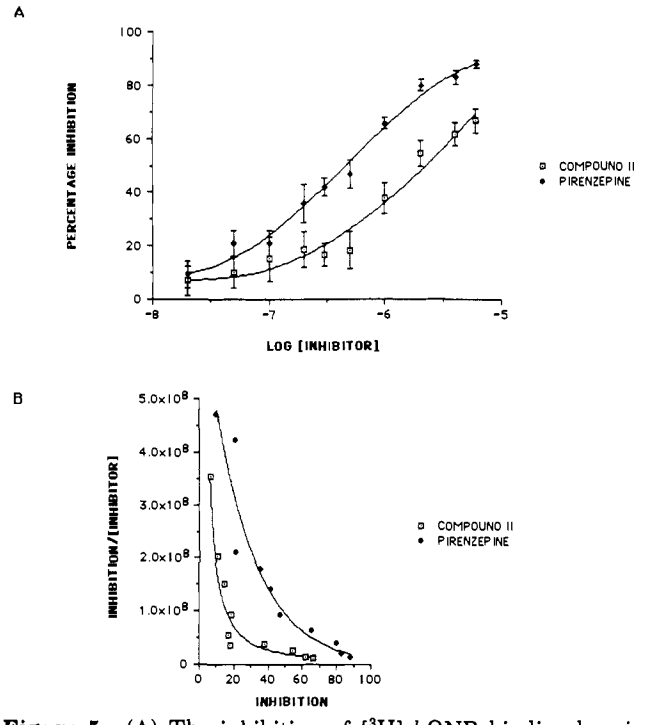

Figure 5. (A) The inhibition of [^{3}H]-*l*-QNB binding by pirenzepine and II in the cerebral cortex. Data represent the mean (±sem) from three animals with 6–12 determinations for each concentration and brain region, (B) Eadie–Hofstee transformation of the data shown in 5A.

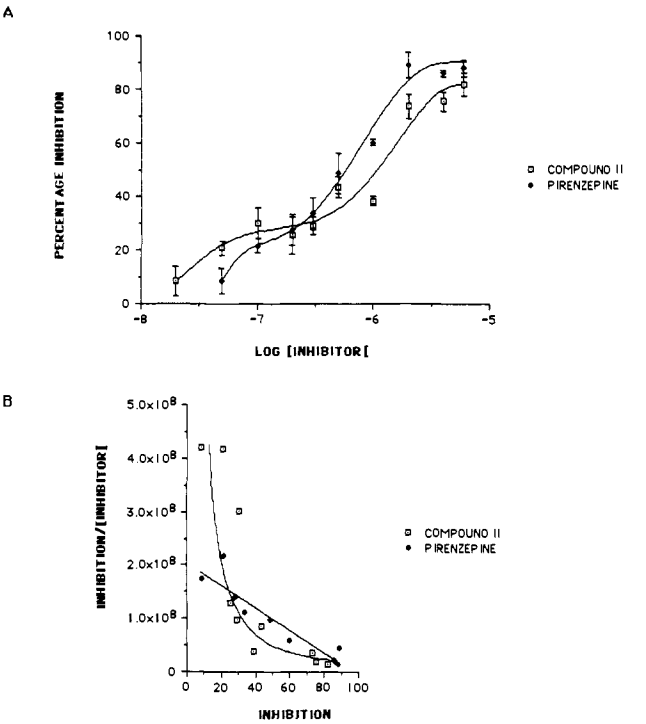

Figure 6. (A) The inhibition of [^{3}H]-*l*-QNB binding by pirenzepine and II in the dorsolateral geniculate. Data represent the mean (±sem) from three animals with three to six determinations for each concentration and brain region, (B) Eadie–Hofstee transformation of the data shown in 6A.

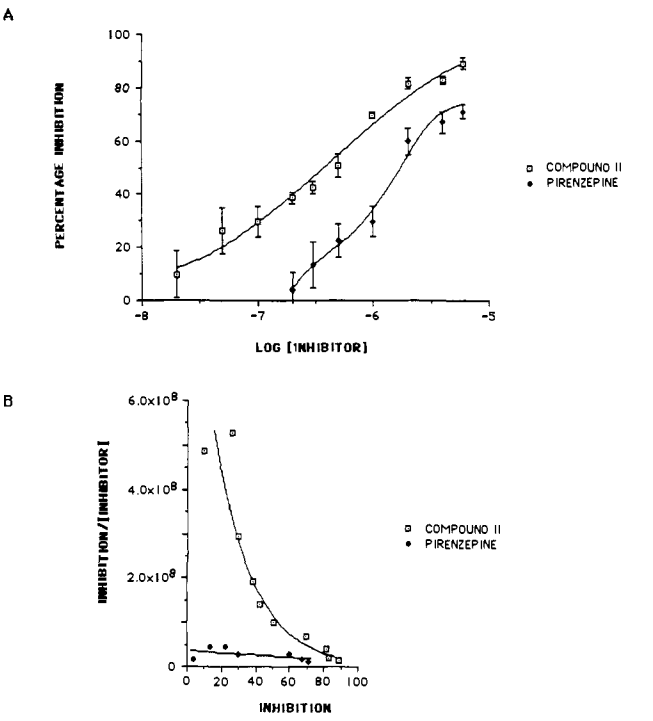

Figure 7. (A) The inhibition of [^{3}H]-*l*-QNB binding by pirenzepine and II in the superior colliculus. Data represent the mean (±sem) from three animals with three to six determinations for each concentration and brain region. (B) Eadie–Hofstee transformation of the data shown in 7A.

receptors.[15,17,19] Other regions of brain, most notably the midline thalamic nuclei, contained populations of receptors with low affinity for both pirenzepine and II. Pharmacologically these receptors in the thalamus resembled the M_2 receptors found in exocrine glands (or M_3) which have been identified in cloning studies to correspond to the m_3 receptor found in the rat.[18,19]

Muscarinic receptors in the cerebellum and hypothalamus possess a high affinity for II in agreement with previous studies using membrane preparations.[13] In addition to muscarinic sites with low affinity for pirenzepine in the midbrain and brain stem, several nuclei displayed a relatively high affinity for both pirenzepine and II. These regions included the substantia nigra, the medial and lateral geniculate nuclei, and the lateral hypothalamus. Pirenzepine affinity for the substantia nigra matched that

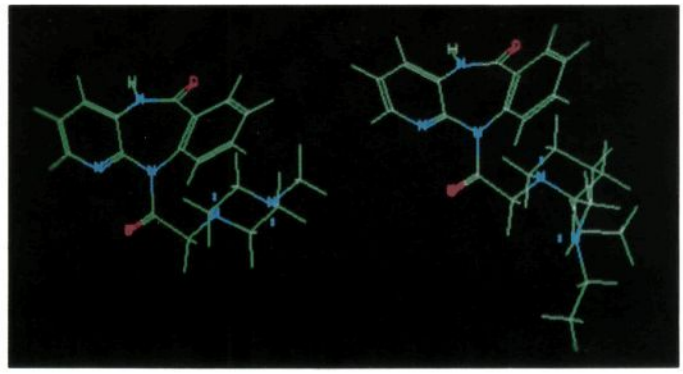

Figure 8. Global conformational minima for pirenzepine and II. The conformations shown possessed the lowest minimum-energy values. The minimum-energy value for pirenzepine was 27.60 kcal/mol while the minimum energy for II was 36.58 kcal/mol.

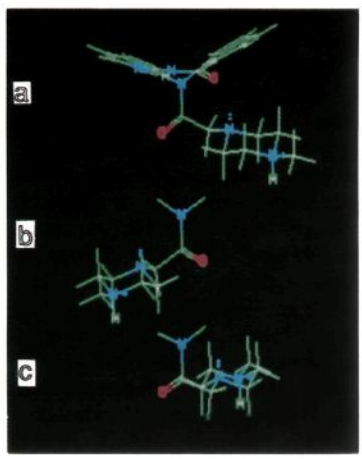

Figure 9. Conformational minima for protonated pirenzepine. The three structures represent conformational minima with an equatorial C21 methyl moiety, which had lower minimum-energy values than the corresponding structures with an axial methyl group. The conformations shown correspond to the conformers described in Table II (a–c). The tricyclic ring system did not vary significantly between the three conformers (RMS < 0.1 Å) and therefore is not pictured for b and c.

found within the hippocampus, yet II was over 10-fold more potent in the substantia nigra than in the hippocampus. Muscarinic receptors in these regions may correspond to the m_4 receptor characterized in cloning studies.[18,19] In situ hybridization studies indicate, however, that the highest density of mRNA for m_4 receptors may be found in the neostriatum which displayed a much lower affinity for II.[28]

The molecular modeling studies presented here consider some potentially important structural features which may confer subtype selectivity for pirenzepine and II. The conformation of the tricyclic ring system did not seem to vary between pirenzepine and compound II or among the three conformations shown in Figure 9 (RMS < 0.1 Å), suggesting that the tricyclic ring system was less important in determining subtype selectivity than the piperazine or piperidine ring conformation and/or orientation.

Three minimum-energy conformations were found for pirenzepine, each with an axial or an equatorial methyl group at N21. Conformations a and b (Figure 9) were interconvertable via rotation around the N(1)–C(16) bond and were of similar energy for both axial and equatorial neutral pirenzepine (Table II). To reach conformation c required a more complex combination of rotations; this structure was more than 2 kcal/mol higher in energy. Protonation of N21 lowered the energies for conformations a and c by 2.0–3.5 kcal/mol. Conformer b, however, *increased* in energy upon protonation. With protonation, conformation a was favored by 3 kcal/mol over both b and c, which were almost equal in energy.

These energy changes were manifested mainly in the electrostatic term, which became 2–4 kcal more stabilizing upon protonation of a or c but remained virtually unchanged in b. The van der Waals interaction term became approximately 2 kcal more stabilizing in a and c but only 1 kcal more stabilizing in b. Some of these gains were off-set by an increase in the torsional strain.

It has been suggested, on the basis of visual analysis of 24 anticholinergic compounds, that there is a single consistent conformation which may be related to biological activity.[20,21] This conformation corresponds to a distance of 5.9 Å between N21 and the center of the pyridine ring. In conformation b of pirenzepine (see Figure 9), which closely resembled this single consistent structure, the N21 to pyridine center distance was 5.0–5.2 Å, depending on axial or equatorial orientation of the methyl group and whether the molecule was neutral or protonated. When this distance in b was constrained to 5.9 Å and the structure was minimized, the energy increased by 9.5 kcal/mol for both the axial and equatorial neutral compounds, even though the geometric changes were small.

Similar studies of the model compound III yielded conformations with the same general orientation although with slightly higher energy minima. The modeling of II was more complex, however, since adding the diethylamino moiety gave eight to ten additional minima for each of the three conformations. The conformer of II corresponding to the pirenzepine conformation noted above would not possess the necessary orientation between the diethylamine and the pyridine ring thought to be important for antimuscarinic activity.[20,21] Other conformations of II may allow the presumed proper orientation of the amine with respect to the pyridine ring, thereby rendering the ligand active at muscarinic receptors. The flexibility of the (diethylamino)methyl side chain would allow the amine to orient in proper relationship with the pyridine ring for antimuscarinic activity while the piperidine ring could prevent the interaction of II with M_1 receptors.

In summary, the modeling data indicate that II was more flexible than pirenzepine, perhaps important for interactions with M_2 receptors. By the same token, the piperazine ring of pirenzepine restricted the movement of the basic nitrogen, perhaps preventing pirenzepine from attaining the conformation necessary for interaction with M_2 receptors. In addition, conformations of II with the proper orientation of the diethylamine and the pyridine ring may interact with muscarinic receptors while the

(28) Brann, M. R.; Buckley, N. J.; Bonner, T. I. *FEBS Lett.* 1988, *230*, 90.

Table II. Calculated Free Energy Values for Pirenzepine and the Compound III Model System. The Structures Indicated Are Shown in Figures 8 and 9

pirenzepine	energy, kcal/mol neutral	energy, kcal/mol protonated	compound III	energy, kcal/mol
conformer a			conformer a	
equatorial	27.60	25.18	equatorial	30.75
axial	30.67	27.54	axial	31.90
conformer b			conformer b	
equatorial	27.74	28.18	equatorial	30.97
axial	30.56	30.78	axial	32.22
conformer c			conformer c	
equatorial	29.90	27.96	equatorial	33.41
axial	32.76	30.41	axial	34.37

position of the piperidine ring in that conformation may prevent binding to M_1 receptors.

The differences in the potency of pirenzepine and II for muscarinic receptor subtypes will help direct studies on the role of muscarinic receptors in mediating the diverse responses to acetylcholine in the central nervous system. In particular, the regional differences in drug binding and receptor populations will provide a strong basis for the interpretation of studies on muscarinic second messenger systems including the stimulation of GTPase,[29] phosphoinositide metabolism,[30] prostaglandin formation,[31] the inhibition of adenylate cyclase,[32,33] and acetylcholine release.[28] The data generated from the current study also will direct efforts for the design and synthesis of novel ligands for muscarinic receptors with possible application in human disorders such as Alzheimer's disease.

Experimental Section

Materials. [^{3}H]-*l*-Quinuclidinyl benzilate ([^{3}H]-*l*-QNB) was purchased from Amersham with a specific activity of 36 Ci/mmol. Tritium standards ([^{3}H]Microscales) [3–100 nCi/mg] also were purchased from Amersham. Pirenzepine and compound II were obtained as gifts from Dr. Karl Thomae, Gmbh. [^{3}H]-Sensitive Ultrofilm was purchased from LKB Industries.

Binding Assays. The methods for measuring inhibition of [^{3}H]-*l*-QNB binding to rat brain slices were adapted from previous studies.[7,9,11,22] Briefly, rats were sacrificed by cardiac perfusion with 50 mL of 40 mM sodium, potassium phosphate buffer, pH 7.4, followed by a light fixative, 0.1% formaldehyde in buffer (200 mL). Each brain was removed rapidly, frozen over liquid nitrogen, and stored at −20 °C until sectioned with a cryostat. Twelve-micrometer-thick coronal sections were taken serially and mounted on acid-washed, subbed (coated with chromium potassium sulfate and gelatin) slides. Slides were stored in microscope slide boxes at −20 °C until used in the binding assay (within 5 days).

Slides were incubated in Coplin jars in the presence of several concentrations of [^{3}H]-*l*-QNB (0.2–2 nM) in buffer for 2.0 h. One jar at each concentration included an excess (1000-fold) of unlabeled atropine to measure nonspecific binding. For the indirect binding assays, slides were incubated with 0.2 nM [^{3}H]-*l*-QNB in the presence of increasing concentrations of unlabeled ligands for 2.0 h. Following the incubation period, sections were rinsed in buffer twice for 10 min. One section from each slide was wiped onto a filter paper and placed in a Nalge bag for standard scintillation counting. The slides were dried and placed back in slide boxes and stored at −20 °C until they were apposed to film. Data analysis included determination of the B_{max} and the apparent dissociation constant [K_d(app)] from Scatchard plots for [^{3}H]-*l*-QNB binding. Inhibition values were determined for each competing ligand. The data were analyzed to generate Hill and Eadie–Hofstee plots.

Film Processing. Slides were apposed to LKB titrium-sensitive Ultrofilm in the dark by placing the slides in film cassettes, pressing the film firmly against the slides, closing the cassette, and wrapping it in a dark cloth for 7–9 days. At the end of the exposure period, the film was developed with Kodak D-19 developer for 5 min, rinsed in a stop bath for 30 s, and fixed with Kodak rapid fixer for another 5 min. After a 20-min rinse in water, the film was dipped in a Photo-flo solution for 30 s and air-dried.

Image Analysis. Images were analyzed with the RAS1000 system developed by Loats Associates for Amersham Corp. Tritium standards ([^{3}H]Microscales) (3–100 nCi/mg) were used for quantifying the autoradiograms. Density readings for standards of known radioactivity were taken for comparison of optical density to isotope levels on each sheet of film. Standard curves for converting optical density to dpm values were best fit by a linear transformation. Background readings of optical density and levels of nonspecific binding were used in determining the relative amount of drug specifically bound to each section for the indirect assays. Several regions of each image were examined for labeling by [^{3}H]-*l*-QNB. The amount of [^{3}H]-*l*-QNB bound to each area was expressed as the mean for each slide (three sections per slide; one or two samples per region). Data taken from areas found in both the left and right hemispheres were pooled from each section to determine the overall mean for that region of brain.

IC_{50} values and Hill slopes were calculated for each region of brain from Hill plots generated from the data on each individual animal (N = 3). The IC_{50} values and Hill slopes were then combined to give a mean (±sem) for each brain region and each antagonist.

Molecular Modeling. Calculations were performed on a VAX 11/785 minicomputer running W. C. Still's program MacroModel. Conformational minima were found with the multiconformer submode[23] using the modified MM2 (85) force field implemented in the program. Explicit calculation of conjugation was not performed; however, aromatic rings and aromatic amides were accounted for by use of special substructure parameters.[24] The pirenzepine conformers (containing both axial and equatorial *N*-methyl groups) were generated as follows. The acyclic torsion angles C2–N1–C16–C17, N1–C16–C17–N18, and C16–C17–N18–C19 were explored in 60° increments over the full 360° circle and the resulting structures were then minimized to a final RMS gradient of <0.05 kJ/Å via the block diagonal Newton–Raphson method with terminal atom movement enabled and then fully minimized to a final RMS gradient of <0.005 kJ/Å by using the full-matrix Newton–Raphson method. All unique conformers within 20 kJ of the global minimum were reported. Protonated species were derived from the final neutral conformations and fully minimized, as described above. A global search about the same torsional angles yielded no low-energy conformations in which intramolecular hydrogen bonding occurred. Hydrogen bonding was indicated if the distance between the H and the acceptor (A) was ≤4 Å and the D–H–A angle was at least 90°. Minimum-energy conformations of the model system III were generated in the same manner as for pirenzepine.

Acknowledgment. This work was supported in part by HEW Grants NS 23929 and NS 25765 and a Research Challenge Grant from the Ohio Board of Reagents. Additional support was supplied by the University of Toledo College of Arts and Sciences Dean's Fund and the Small Grants Research Fund.

Registry No. I, 102394-31-0; II, 28797-61-7.

(29) Ghodsi, S.; Messer, W. S., Jr.; Hoss, W. *Soc. Neurosci. (abstr)* **1987**, *13*, 1374.
(30) Fisher, S. K.; Klinger, P. D.; Agranoff, B. W. *J. Biol. Chem.* **1983**, *258*, 7358.
(31) Reichman, M.; Nen, W.; Hokin, L. E. *Biochem. Biophys. Res. Commun.* **1987**, *146*, 1256.
(32) Olianas, M. C.; Onali, P.; Neff, N. H.; Costa, E. C. *Mol. Pharmacol.* **1983**, *23*, 393.
(33) Gil, D. W.; Wolfe, B. B. *J. Pharmacol. Exp. Ther.* **1985**, *232*, 608.